

# Theoretical study of the $\Lambda(1520)$ photoproduction off proton target based on the new CLAS data

Jun He<sup>a,b,c</sup>

<sup>a</sup>*Research Center for Hadron and CSR Physics, Lanzhou University and Institute of Modern Physics of CAS, Lanzhou 730000, China*

<sup>b</sup>*Theoretical Physics Division, Institute of Modern Physics, Chinese Academy of Sciences, Lanzhou 730000, China*

<sup>c</sup>*State Key Laboratory of Theoretical Physics, Institute of Theoretical Physics, Chinese Academy of Sciences, Beijing 100190, China*

---

## Abstract

Based on the high precision experimental data released by the CLAS Collaboration recently, the interaction mechanism of the photoproduction of  $\Lambda(1520)$  off a proton target is investigated within a Regge-plus-resonance approach. With the decay amplitudes predicted in the constituent quark model, the roles played by nucleon resonances are studied. It is found that  $N(2120)$  provides the most important contribution among the nucleon resonances predicted in the constituent quark model. The  $t$  channel contribution with Regge trajectories and the  $\Lambda$  intermediate  $u$  channel are responsible to the behaviors of the differential cross section at forward and backward angles, respectively.

**Keywords:**  $\Lambda(1520)$  photoproduction, nucleon resonance, effective Lagrangian, constituent quark model

---

## 1. Introduction

Recently, the CLAS Collaboration at Jefferson National Accelerator Facility released their exclusive photoproduction cross sections for the  $\Lambda(1520)$ ,  $\Sigma^0(1385)$  and  $\Lambda(1405)$  for energies from near threshold up to a center of mass energy  $W$  of 2.85 GeV with large range of the  $K$  production angle [1] (labeled as CLAS13 in this work). Since threshold for the photoproduction of  $\Lambda(1520)$  is about 2.01 GeV, the new experimental data with high precision released by the CLAS Collaboration provide an opportunity to study the nucleon resonances above 2 GeV.

Among about two dozen nucleon resonances predicted by the constituent quark model, a  $D_{13}$  state  $N(2120)$  with two star, which is labeled as  $N(2080)$  in the previous version of Particle Data Group (PDG) [2, 3], should play the most important role in the photoproduction of  $\Lambda(1520)$  off proton target due to its large decay widths in  $\gamma p$  and  $\Lambda(1520)N$  channels predicted in the constituent quark model [4, 5].  $N(2120)$  has attracted much attentions due to its importance found in many channels, such as  $\gamma p \rightarrow K^*\Lambda$  [6],  $\phi$  photoproduction [7] and  $\eta'p/\eta p$  photoproduction [8, 9, 10, 11]. A new bump structure was found at  $W \simeq 2.1$  GeV

in the differential cross sections for the photoproduction of  $\Lambda(1520)$  at forward angles measured by LEPS Collaboration at energies from near threshold up to 2.4 GeV [12] (labeled as LEPS10), which could be reproduced by including the resonance  $N(2120)$  [13, 14].

In Refs. [13, 14], the photoproduction of  $\Lambda(1520)$  has been investigated based on the LEPS10 data and the differential cross sections are well reproduced. However, only the differential cross sections at forward angles are measured in the LEPS10 experiment. At forward angles the  $t$  channel contribution is dominant while the  $u$  channel contribution is negligible. Besides, the contribution from  $N(2120)$  is expected to be important at all kaon production angles. Hence it is interesting to study the interaction mechanism of the  $\Lambda(1520)$  photoproduction, especially the  $u$  channel and nucleon resonance intermediate  $s$  channel, with the CLAS13 data with large range of the kaon production angle. In a recent work, the  $u$  channel contribution is found important at the backward angles [15]. However the differential cross sections at forward angles are not so well reproduced. In an analysis of the CLAS13 data for  $\Sigma(1385)$  photoproduction the Regge trajectory is found essential to reproduce the behavior of the differential cross sections at forward angles [16]. In this work we will study the  $\Lambda(1520)$  photoproduction off proton target in a Regge-plus-resonance approach based on the new CLAS13 data to explore the interaction mechanism of the  $\Lambda(1520)$  photoproduction.

This paper is organized as follows. After introduction, we will present the effective Lagrangian and Regge trajectory used in this work. The experimental data will be fitted and the theoretical results of the differential and total cross sections compared with experiment will be given in Sec. 3. Finally the paper ends with a brief summary.

## 2. Formula

The photoproduction of  $\Lambda(1520)$  off proton target with  $K$  occurs through the following diagrams in Fig. 1.

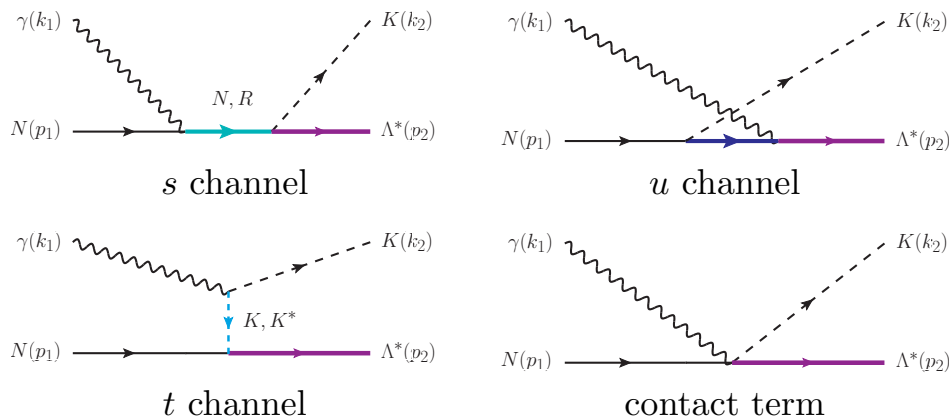


Figure 1: (Color online) The diagrams for the  $s$ ,  $u$ ,  $t$  channels and the contact term.

The Lagrangians use in the Born terms are given below [13, 14, 17]

$$\begin{aligned}
\mathcal{L}_{\gamma KK} &= ieQ_K [(\partial^\mu K^\dagger)K - (\partial^\mu K)K^\dagger] A_\mu, \\
\mathcal{L}_{\gamma NN} &= -e\bar{N} \left[ Q_N \not{A} - \frac{\kappa_N}{4M_N} \sigma^{\mu\nu} F^{\mu\nu} \right] N, \\
\mathcal{L}_{KN\Lambda^*} &= \frac{g_{KN\Lambda^*}}{M_K} \bar{\Lambda}^{*\mu} \partial_\mu K \gamma_5 N + \text{H.c.}, \\
\mathcal{L}_{\gamma KN\Lambda^*} &= -\frac{ieQ_N g_{KN\Lambda^*}}{M_K} \bar{\Lambda}^{*\mu} A_\mu K \gamma_5 N + \text{H.c.},
\end{aligned} \tag{1}$$

where  $F^{\mu\nu} = \partial^\mu A^\nu - \partial^\nu A^\mu$  with  $A^\mu$ ,  $N$ ,  $K$ ,  $\Lambda^*$  are the fields for the photon, nucleon, kaon and  $\Lambda^*(1520)$ .  $M_N$  and  $M_K$  are the masses of the nucleon and  $K$  meson.  $Q_h$  is the charge of the hadron in the unit of  $e = \sqrt{4\pi\alpha}$ . The anomalous magnetic momentum  $\kappa_N = 1.79$  for proton. With the decay width of  $\Lambda^* \rightarrow NK$  in Particle Data Group (PDG) [2], the coupling constant can be obtained as  $g_{KN\Lambda^*} = 10.5$ .

The  $u$ -channel diagram contains intermediate hyperon  $Y$  with spin- $1/2$  as shown in Fig. 1. The effective Lagrangians for this diagram are

$$\begin{aligned}
\mathcal{L}_{KNY} &= \frac{g_{KNY}}{M_N + M_Y} \bar{N} \gamma^\mu \gamma_5 Y \partial_\mu K + \text{H.c.}, \\
\mathcal{L}_{\Lambda^* Y \gamma} &= -\frac{ie f_1^u}{2M_Y} \bar{Y} \gamma_\nu \gamma_5 F^{\mu\nu} \Lambda_\mu^* + \frac{e f_2^u}{(2M_Y)^2} \partial_\nu \bar{Y} \gamma_5 F^{\mu\nu} \Lambda_\mu^* + \text{H.c.},
\end{aligned} \tag{2}$$

where  $F_{\mu\nu} = \partial_\mu A_\nu - \partial_\nu A_\mu$ . For the intermediate  $\Lambda$  state, the coupling constants  $f_1^u = -7.22$  and  $f_2^u = 9.48$  can be obtained from the ratio of the helicity amplitudes  $A_{3/2} = -122$  and  $A_{1/2} = 13$  predicted in the constituent quark model [20] and the PDG decay width  $\Gamma_\gamma = 133$  keV [2]. This method has been used in Ref. [19] to determine the coupling constants for  $\Sigma(1385) \rightarrow \Lambda\gamma$ . The coupling constant  $g_{KN\Lambda}$  can be determined by flavor SU(3) symmetry, which gives value  $g_{KN\Lambda} = -13.24$  [19]. The  $\Sigma$  exchange is negligible due to the small coupling constant determined from SU(3) symmetry [19].

It is well known that the amplitudes from nucleon intermediate  $s$  channel, the  $K$  exchange  $t$  channel and the contact term are not gauge invariant while for the sum of three amplitudes the gauge invariance can be guaranteed. If the form factor which reflects the hadron internal structure is included, the gauge invariance will be violated. To restore the gauge invariance, a generalized contact term is introduced as [18, 19]

$$\begin{aligned}
M_c^{\mu\nu} &= \frac{ieg_{KN\Lambda^*}}{m_K} \gamma_5 \left[ g^{\mu\nu} F_t + k_2^\mu (2k_2 - k_1)^\nu \frac{(F_t - 1)[1 - h(1 - F_s)]}{t - m_K^2} \right. \\
&\quad \left. + k_2^\mu (2p_1 - k_1)^\nu \frac{(F_s - 1)[1 - h(1 - F_t)]}{s - M_N^2} \right],
\end{aligned} \tag{3}$$

where the  $h$  is free parameter and will be fitted by the experimental data.

In this work, we adopt the form factor with form,

$$F(q^2) = \left( \frac{n\Lambda^4}{n\Lambda^4 + (q^2 - M^2)^2} \right)^n, \tag{4}$$

where  $M$  and  $q$  are the mass and momentum of the off-shell intermediate particle. In this work, except  $n = 2$  for  $K^*$  exchange, we choose  $n = 1$  for other channels as Ref. [16]. The cut-off  $\Lambda$  will be set as free parameter in this work.

It is well known that the behavior of the cross section for the photoproduction at high photon energy is described by Regge trajectory. We introduce the pseudoscalar and vector strange-meson Regge trajectories following [21, 22, 23]:

$$\begin{aligned}\frac{1}{t - m_K^2} \rightarrow \mathcal{D}_K &= \left( \frac{s}{s_{scale}} \right)^{\alpha_K} \frac{\pi \alpha'_K}{\Gamma(1 + \alpha_K) \sin(\pi \alpha_K)}, \\ \frac{1}{t - m_{K^*}^2} \rightarrow \mathcal{D}_{K^*} &= \left( \frac{s}{s_{scale}} \right)^{\alpha_{K^*} - 1} \frac{\pi \alpha'_{K^*}}{\Gamma(\alpha_{K^*}) \sin(\pi \alpha_{K^*})},\end{aligned}\quad (5)$$

where  $\alpha'_{K,K^*}$  is the slope of the trajectory.  $\alpha_{K,K^*}$  is the linear trajectory, which is a function of  $t$  as  $\alpha_K = 0.70 \text{ GeV}^{-2}(t - m_K^2)$ ,  $\alpha_{K^*} = 1 + 0.85 \text{ GeV}^{-2}(t - m_{K^*}^2)$ . The scale constant  $s_{scale}$  is set as  $1 \text{ GeV}^2$ . The coupling constant for Regge trajectory  $\bar{g}_{KN\Lambda}^{Reg} = k^R g_{KN\Lambda^*}$  should be different from the one for the real  $K$  exchange  $g_{KN\Lambda^*} = 10.5$  [13, 14, 17]. In this work we set it as free parameter. We expect this difference should not be very large. The  $k^R$  for  $K^*$  exchange is set to 1 considered that its contribution is small compared with  $K$  exchange contribution [14].

The Regge trajectories should work completely at high photon energies and interpolate smoothly to a  $K$  or  $K^*$  exchange at low energies. Toki *et al.* [24] and Nam and Kao [17] introduced a weighting function to describe such picture. Here we adopt the treatment as [16],

$$\frac{F_t}{t - m_K^2} \rightarrow \frac{F_t}{t - m_K^2} \mathcal{R} = \mathcal{D}_K R + \frac{F_t}{t - m_K^2} (1 - R), \quad (6)$$

where  $R = R_s R_t$  with

$$R_s = \frac{1}{2} \left[ 1 + \tanh \left( \frac{s - s_{Reg}}{s_0} \right) \right], \quad R_t = 1 - \frac{1}{2} \left[ 1 + \tanh \left( \frac{|t| - t_{Reg}}{t_0} \right) \right]. \quad (7)$$

The free parameters  $s_{Reg}$ ,  $s_0$ ,  $t_{Reg}$  and  $t_0$  will be determined by fitting experimental data.

The adoption of Regge trajectory will violate the gauge invariance also. To restore the gauge invariance, we redefine the relevant amplitudes as follow,

$$i\mathcal{M}_t + i\mathcal{M}_s + i\mathcal{M}_c \rightarrow i\mathcal{M}_t^{\text{Regge}} + (i\mathcal{M}_s + i\mathcal{M}_c)\mathcal{R}. \quad (8)$$

The Lagrangians for the resonances with arbitrary half-integer spin are [14, 19, 25, 26, 27],

$$\mathcal{L}_{\gamma NR(\frac{1}{2}^\pm)} = \frac{ef_2}{2M_N} \bar{N} \Gamma^{(\mp)} \sigma_{\mu\nu} F^{\mu\nu} R + \text{H.c.}, \quad (9)$$

$$\begin{aligned}\mathcal{L}_{\gamma NR(J^\pm)} &= \frac{-i^n f_1}{(2M_N)^n} \bar{N} \gamma_\nu \partial_{\mu_2} \cdots \partial_{\mu_n} F_{\mu_1\nu} \Gamma^{\pm(-1)^{n+1}} R^{\mu_1\mu_2\cdots\mu_n} \\ &+ \frac{-i^{n+1} f_2}{(2M_N)^{n+1}} \partial_\nu \bar{N} \partial_{\mu_2} \cdots \partial_{\mu_n} F_{\mu_1\nu} \Gamma^{\pm(-1)^{n+1}} R^{\mu_1\mu_2\cdots\mu_n} + \text{H.c.},\end{aligned}\quad (10)$$

$$\mathcal{L}_{RK\Lambda^*} = \frac{ig_2}{2m_K} \partial_\mu K \bar{\Lambda}_\mu^* \Gamma^{(\pm)} R, + \text{H.c.}, \quad (11)$$

$$\begin{aligned} \mathcal{L}_{RK\Lambda^*} &= \frac{-i^{n+1}g_1}{m_K^n} \bar{\Lambda}_{\mu_1}^* \gamma_\nu \partial_\nu \partial_{\mu_2} \cdots \partial_{\mu_n} K \Gamma^{\pm(-1)^n} R^{\mu_1\mu_2\cdots\mu_n} \\ &+ \frac{-i^n g_2}{m_K^{n+1}} \bar{\Lambda}_\alpha^* \partial_\alpha \partial_{\mu_1} \partial_{\mu_2} \cdots \partial_{\mu_n} K \Gamma^{\pm(-1)^n} R^{\beta\mu_1\mu_2\cdots\mu_n} + \text{H.c.}, \end{aligned} \quad (12)$$

where  $R_{\mu_1\cdots\mu_n}$  is the field for the resonance with spin  $J = n + 1/2$ , and  $\Gamma^{(\pm)} = (\gamma_5, 1)$  for the different resonance parity. The coupling constants  $f_1$ ,  $f_2$ ,  $g_1$  and  $g_2$  can be determined by the helicity amplitudes  $A_{1/2,3/2}$  and decay amplitudes  $G(\ell_1, \ell_2)$  predicted in the constituent quark model [4, 5]. The interested reader is referred to Refs. [14, 16, 19].

### 3. Results

With the formula given above, the CLAS13 and/or LEPS10 data for the differential cross section of the  $\Lambda(1520)$  photoproduction will be fitted with the contributions from the nucleon and nucleon resonance intermediate  $s$  channels, the  $K$  and  $K^*$  exchange  $t$  channels, the  $\Lambda$  intermediate  $u$  channel and the contact term. The fitting is done with the help of the MINUIT code in the cernlib.

#### 3.1. Fitting procedure

In our model, the nucleon intermediate  $s$  channel,  $K$  and  $K^*$  exchange  $t$  channels with Regge trajectory,  $\Lambda$  intermediate  $u$  channel and contact term are considered. The involved parameters are listed in Table 1. The best fitted values with the uncertainties of the parameters through fitting both CLAS13 and LEPS10 data are also presented.

Table 1: The predetermined parameters and fitted parameters. The mass, width and cut offs are in the unit of GeV. The parameters for Regge trajectory are in the unit of  $\text{GeV}^2$ .

Predetermined parameters							
$g_{\gamma KK}$	0.254	$g_{KN\Lambda^*}$	10.5	$g_{K^*N\Lambda^*}$	20	$g_{KN\Lambda}$	-13.24
$f_1^u$	-7.2	$f_2^u$	9.5	$\Gamma_R$	330		
fitted parameters							
$\sqrt{s_{Reg}}$	$2.23 \pm 0.08$	$s_0$	$0.30 \pm 0.70$	$\sqrt{t_{Reg}}$	$1.71 \pm 0.97$	$t_0$	$0.65 \pm 1.05$
$\Lambda_{s,K}$	$0.60 \pm 0.10$	$\Lambda_u$	$0.55 \pm 0.08$	$\Lambda_{K^*}$	$0.79 \pm 0.64$	$\Lambda_R$	$0.70 \pm 0.25$
$k^R$	$0.74 \pm 0.01$	$h$	$1.02 \pm 0.02$				

In Table. 2, the correlation coefficient of the best fitted parameters is also presented. The  $\Lambda_{s,K}$  and  $\Lambda_{K^*}$  have high correlation, which indicates the contributions from  $K$  and  $K^*$  exchange play a similar role in the reproduction of the experimental data.

Table 2: Parameter correlation coefficients.

	$\sqrt{s_{Reg}}$	$s_0$	$\sqrt{t_{Reg}}$	$t_0$	$\Lambda_{s,K}$	$h$	$\Lambda_u$	$\Lambda_{K^*}$	$\Lambda_R$	$k^R$
$\sqrt{s_{Reg}}$	1.000	0.009	0.062	-0.052	-0.532	-0.371	-0.198	0.490	0.470	-0.003
$s_0$	0.009	1.000	0.001	0.000	-0.009	-0.006	-0.005	0.008	0.013	0.011
$\sqrt{t_{Reg}}$	0.062	0.001	1.000	0.507	-0.086	-0.521	0.042	0.088	-0.118	-0.039
$t_0$	-0.052	0.000	0.507	1.000	0.057	0.180	-0.246	-0.093	0.212	-0.001
$\Lambda_{s,K}$	-0.532	-0.009	-0.086	0.057	1.000	0.507	0.279	-0.983	-0.168	-0.005
$h$	-0.371	-0.006	-0.521	0.180	0.507	1.000	-0.095	-0.526	-0.059	0.024
$\Lambda_u$	-0.198	-0.005	0.042	-0.246	0.279	-0.095	1.000	-0.252	-0.442	-0.018
$\Lambda_{K^*}$	0.490	0.008	0.088	-0.093	-0.983	-0.526	-0.252	1.000	0.106	0.004
$\Lambda_R$	0.470	0.013	-0.118	0.212	-0.168	-0.059	-0.442	0.106	1.000	0.008
$k^R$	-0.003	0.011	-0.039	-0.001	-0.005	0.024	-0.018	0.004	0.008	1.000

The nucleon resonances should be important at energies near threshold of the  $\Lambda(1520)$  photoproduction. In the constituent quark model a large amount of nucleon resonances in the energy region considered in this work are predicted, which will make the fitting very difficult. In this work we use the following criterion to select the nucleon resonances which will be considered in the fitting,

$$\lambda = (A_{1/2}^2 + A_{3/2}^2)(G(\ell_1)^2 + G(\ell_2)^2) \cdot 10^5 > 0.01. \quad (13)$$

According to such criterion only six resonances survive as listed in Table. 3. Estimated from the values of  $\lambda$ ,  $N(2120)$  with  $\lambda = 2.14$  should be the most important one among all nucleon resonances considered in the current work.

Table 3: The nucleon resonances considered. The mass  $m_R$ , helicity amplitudes  $A_{1/2,3/2}$  and partial wave decay amplitudes  $G(\ell)$  are in the unit of MeV,  $10^{-3}/\sqrt{\text{GeV}}$  and  $\sqrt{\text{MeV}}$ , respectively. The last column is for  $\chi^2$  after turning off the corresponding nucleon resonance and refitting.  $\chi^2 = 3.05$  in the full model. The amplitudes are from Refs. [4, 5].

State	PDG	$A_{1/2}^p$	$A_{3/2}^p$	$G(\ell_1)$	$G(\ell_2)$	$\lambda$	$\chi^2$
$[N_{\frac{1}{2}}^{-}]_3(1945)$	$N(1895)$	12		$6.4^{+5.7}_{-6.4}$		0.59	3.04
$[N_{\frac{3}{2}}^{-}]_3(1960)$	$N(2120)$	36	-43	$-2.6^{+2.6}_{-2.8}$	$-0.2^{+0.2}_{-1.3}$	2.14	3.54
$[N_{\frac{5}{2}}^{-}]_2(2080)$	$N(2060)$	-3	-14	$-4.7^{+4.7}_{-1.2}$	$-0.3^{+0.3}_{-0.8}$	0.45	3.00
$[N_{\frac{5}{2}}^{-}]_3(2095)$		-2	-6	$-2.4^{+2.4}_{-2.0}$	$-0.1^{+0.1}_{-0.3}$	0.02	3.05
$[N_{\frac{7}{2}}^{-}]_1(2090)$	$N(2190)$	-34	28	$-0.5^{+0.4}_{-0.6}$	$0.0^{+0.0}_{-0.0}$	0.05	3.06
$[N_{\frac{7}{2}}^{+}]_2(2390)$		-14	-11	$3.1^{+0.8}_{-1.2}$	$0.3^{+0.3}_{-0.2}$	0.31	3.14

In the fitting procedure, the values of the nucleon resonance masses suggested in PDG [2] are preferred. For the nucleon resonances which is not listed in PDG, the prediction of the constituent quark model will be adopted. To avoid the proliferation of the free parameters, the Breit-Wigner widths for all nucleon resonances are set to 330 MeV, which is consistent to the values suggested in PDG for the nucleon resonances listed in Table. 3 [2]. Here, we would like to mention that with the help of the helicity and decay amplitudes listed in Table. 3 the contributions from nucleon resonances are only dependent on one free parameter  $\Lambda_R$ , which is also presented in Table 1.

With the parameters listed in Table 1, the experimental data about the differential cross section will be fitted. In the fitting procedure, we only consider CLAS13 and LEPS10 data. The reduced  $\chi^2$  per degree of freedom are presented in Table 4. The corresponding values of fitted parameters are listed in Table 1. Here only statistic uncertainties are included in the fitting procedure. To compare with Ref. [15], the results with systematic uncertainty  $\sigma_{sys} = 11.6\%$  and  $5.92\%$  for CLAS13 and LEPS10, are also listed in Table 4. The results with only CLAS13 data are also presented for comparison.

Table 4: The reduced  $\chi^2$  for the full model and the models after turning off  $u$  channel, all nucleon resonances, the nucleon resonances except  $N(2120)$  the Regge trajectory or the  $K^*$  exchange and refitting. The second to forth columns are for the results with both CLAS13 and LEPS10 data. The last three columns are for the results with CLAS13 data only. The second (five) and third (sixth) columns are for the results with and without systematic uncertainties  $\sigma_{sys}$ .

	CLAS13&LEPS10			CLAS13		
	no $\sigma_{sys}$	with $\sigma_{sys}$	Ref. [15]	no $\sigma_{sys}$	with $\sigma_{sys}$	Ref. [15]
Full model	3.05	[1.38]	[2.5]	2.65	[1.07]	[2.5]
no $u$ channel	4.10	[2.08]	[9.9]	4.08	[2.13]	[5.6]
no $N^*$	4.82	[2.12]	[3.0]	4.79	[2.22]	[3.0]
only $N(2120)$	3.27	[1.48]		2.85	[1.08]	
no Regge	8.39	[2.95]		7.69	[2.51]	
no $K^*$	3.36	[1.51]		2.89	[1.18]	

For the full model  $\chi^2 = 3.05$  and decreases to 1.38 if the systematic uncertainty are included, which is much smaller than  $\chi^2 = 2.5$  in Ref. [15]. If LEPS10 data is excluded,  $\chi^2$  decreases to 2.65. If turning off  $\Lambda$  intermediate  $u$  channel,  $\chi^2$  increases to 4.10, which suggests the importance of the  $u$  channel contribution. After excluding all nucleon resonances,  $\chi^2$  increases to 4.82. However, if  $N(2120)$  is included,  $\chi^2$  decreases to 3.27, which is close to 3.05 with full model. The result shows that  $N(2120)$  is dominant in the nucleon resonance contribution. The importance of  $N(2120)$  can be also observed in Table 3. After turning off  $N(2120)$  the corresponding  $\chi^2$  is 3.54, which is much larger other nucleon resonances as the value of  $\lambda = 2.14$  for  $N(2120)$ . We also check the importance of the Regge trajectory. A value of  $\chi^2$  about 8 is found if the Regge trajectory is turned off. If the systematic uncertainty are included,  $\chi^2$  is 2.95, which is close to the  $\chi^2 = 2.5$  in Ref. [15]. Compared with  $\chi^2 = 3.05$

for the full model, the Regge trajectory is essential to describe the experimental differential cross section. To check the correlation of the contributions from the  $K$  exchange and  $K^*$  exchange, the  $\chi^2$  after turning  $K^*$  exchange are also presented. It is found that the absence of  $K^*$  contribution is compensated by the  $K$  contribution as suggested by the high correlation between  $\Lambda_{s,K}$  and  $\Lambda_{K^*}$  in Table 2.

### 3.2. Differential cross section

Compared with the reduced  $\chi^2$ , the explicit differential cross section can provide more information about interaction mechanism of  $\Lambda(1520)$  photoproduction. First, we present our results for CLAS13 and CLAS10 data which are used in the fitting procedure.

In Fig. 2, the differential cross sections compared with CLAS13 data are figured. The LEPS10 data at same energies are also plotted in the corresponding subfigure. One can find

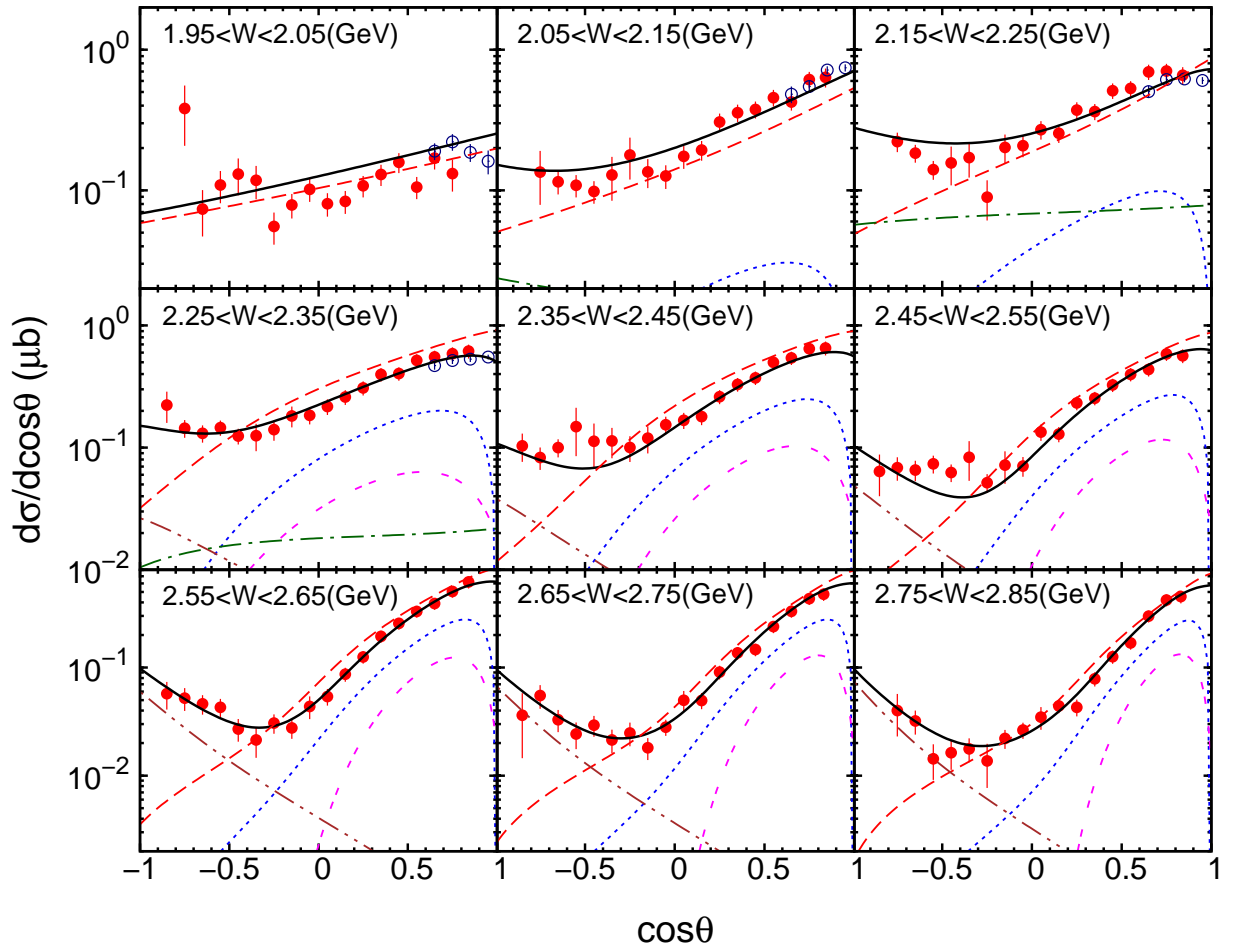


Figure 2: (Color online) The differential cross section  $d\sigma/d\cos\theta$  with variation of  $\cos\theta$ . The full (black), dashed (red), dotted (blue), dash-dot-dotted (brown), dash-dashed (magenta) and dash-dotted (darkgreen) lines are for full model, contact term,  $K$  exchange  $t$  channel,  $u$  channel,  $K^*$  exchange  $t$  channel and  $N(2120)$ . The full circle (red) and open circle (blue) are for CLAS13 data [1] and LEPS10 data [12].



that experimental data are well reproduced in our model at all energies and angles. The dominant contributions are from Born terms, among which the contact term plays the most important role. At the low energy the  $K$  exchange contribution is smaller and becomes more important at high energies (please note here and hereafter that the amplitude of the contact term, the  $K$  exchange, or the  $s$  channel is not gauge invariant. Here, the result is obtained in the center of mass frame). The vector meson  $K^*$  exchange provides considerable contribution at high energies. Compared with Fig.3 in Ref. [15], the Regge trajectory is important to reproduce the behavior of the differential cross section at forward angles especially at high energies. The  $u$  channel is responsible to the increase of the differential cross section with the decrease of  $\cos\theta$  at high energies. However, the similar increase at low energies is from  $N(2120)$  contribution instead.

The results compared with LEPS10 data are figured in Fig. 3. The CLAS13 data at same angles are also plotted. One can find that there exist discrepancies between LEPS10

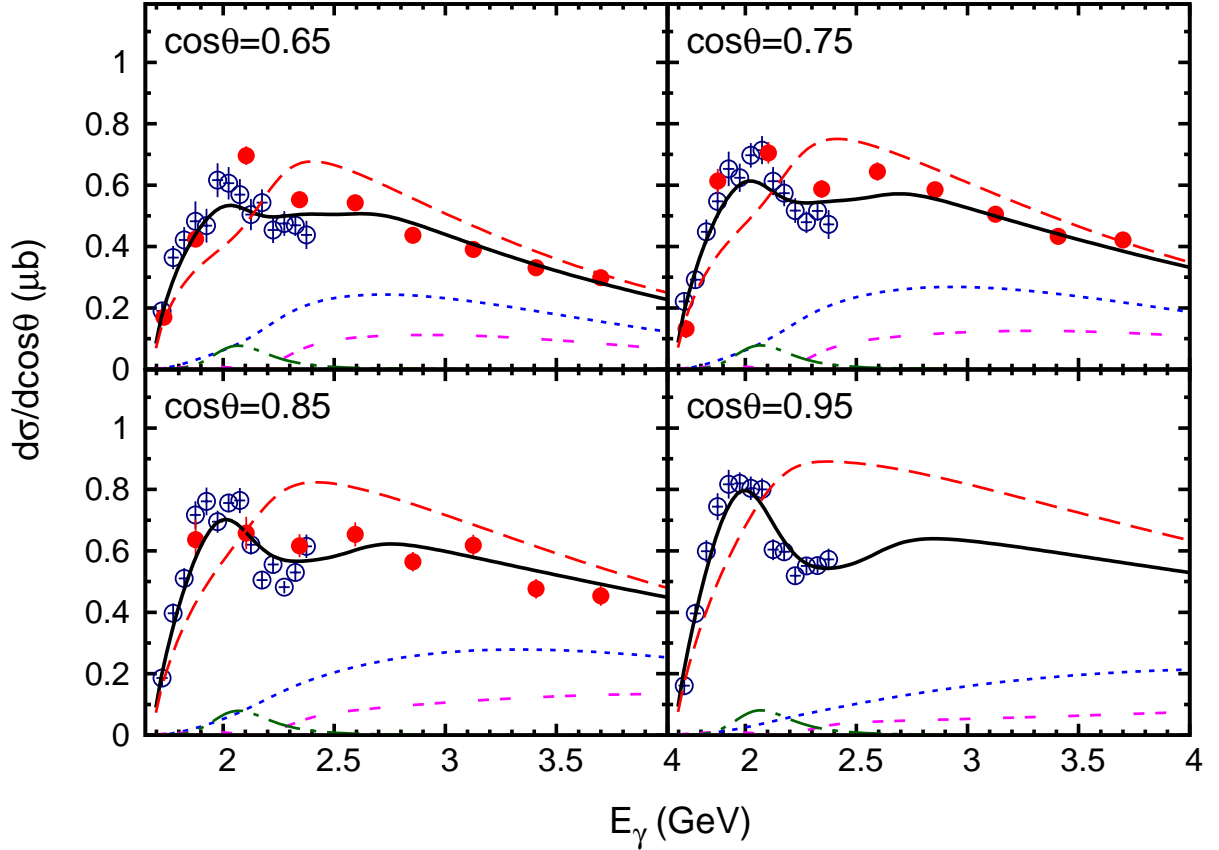


Figure 3: (Color online) The differential cross section  $d\sigma/d\cos\theta$  with the variation of the photon energy  $E_\gamma$  compared with LEPS10 data. The notation as Fig. 2.

data and CLAS13 data especially at  $\cos\theta = 0.65$ . Our results are close to the LEPS10 data and the bump structure is well reproduced with the contribution from  $N(2120)$ . The

contact term contribution is dominant at energies from near threshold up to  $E_\gamma = 4$  GeV. Generally, the CLAS13 data is reproduced especially at high energies. Compared with Fig.4 in Ref. [15] a large difference can be found in the prediction of the differential cross section at extreme forward angle  $\cos\theta = 0.95$ . A sharp increase was predicted at energies larger than 2.5 GeV in Ref. [15] while our result suggests a smooth heave. The difference should be from adoption of Regge trajectory in the current work which is not considered in Ref. [15]. It can be checked in the future experiment.

In the fitting, the polarization asymmetry measured in LEPS10 experiment are not included. As shown in the previous work [13, 14], the sign of the polarization asymmetry should be reversed compared with the experiment. The results in this work confirm the previous conclusion as shown in Fig. 4.

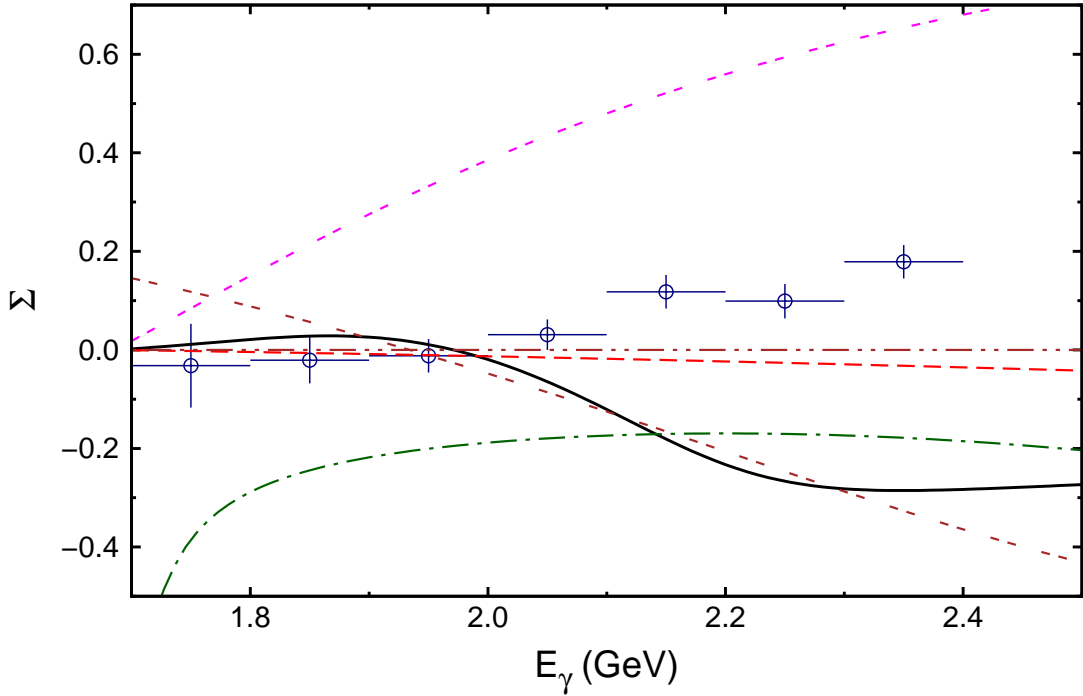


Figure 4: (Color online) Polarization asymmetry with the variation of the energy of photon  $E_\gamma$  compared with LEPS10 data [12]. The notation as Fig. 2.

To show a picture around the resonance pole of  $N(2120)$ , the  $d\sigma/d\cos\theta$  against  $\theta$  at 2.2 GeV is calculated and compared with LEPS09 data in Ref. [28] which are not included in the fitting procedure. As shown in Fig. 5, the experimental data are reproduced generally in our model. The general shape for the differential cross section against  $\theta$  is mainly formed by the contact term contribution. The slow increase at backward angles is from  $N(2120)$  contribution. For differential cross section with the variation of  $E_\gamma$ ,  $N(2120)$  provides contribution comparable with the contact term at backward angles and is responsible to the bump structure.

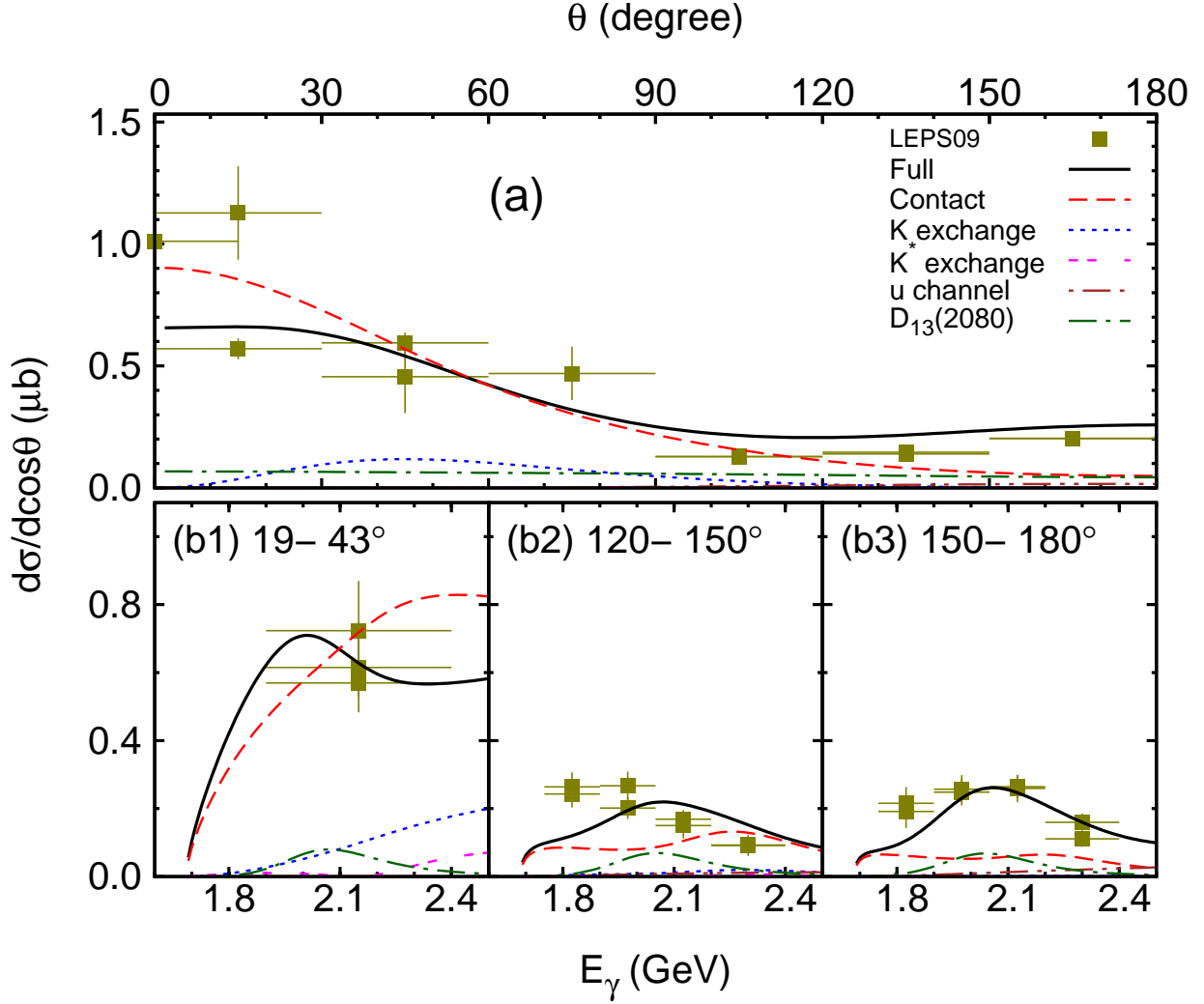


Figure 5: (Color online) (a) The differential cross section  $d\sigma/d\cos\theta$  with the variation of  $\theta$  at photon energy 2.2 GeV compared with the LEPS09 data at photon energy 1.9-2.4 GeV. (b1-b3) The differential cross section  $d\sigma/d\cos\theta$  with the variation of photon energy  $E_\gamma$ . the notation as in Fig. 2. The experimental data are from Ref. [28].

Recently CLAS Collaboration reported their preliminary results about the photoproduction of  $\Lambda(2120)$  off both proton and neutron in deuterium at the photon energy from 1.87 to 5.5 GeV in the *eg3* run [29]. We do not consider these preliminary *eg3* data in the fitting procedure. However, we still present our theoretical results from 1.87 to 5.5 GeV to show the interaction mechanism at higher energies. As shown in Fig. 6, our theoretical results are consistent with the preliminary *eg3* data especially the later one. The contribution from the contact term plays most important role at the energies from threshold up to 5.5 GeV while the contributions from nucleon resonances decreases rapidly at the photon energy large than the energy point corresponding to the Breit-Wigner mass.

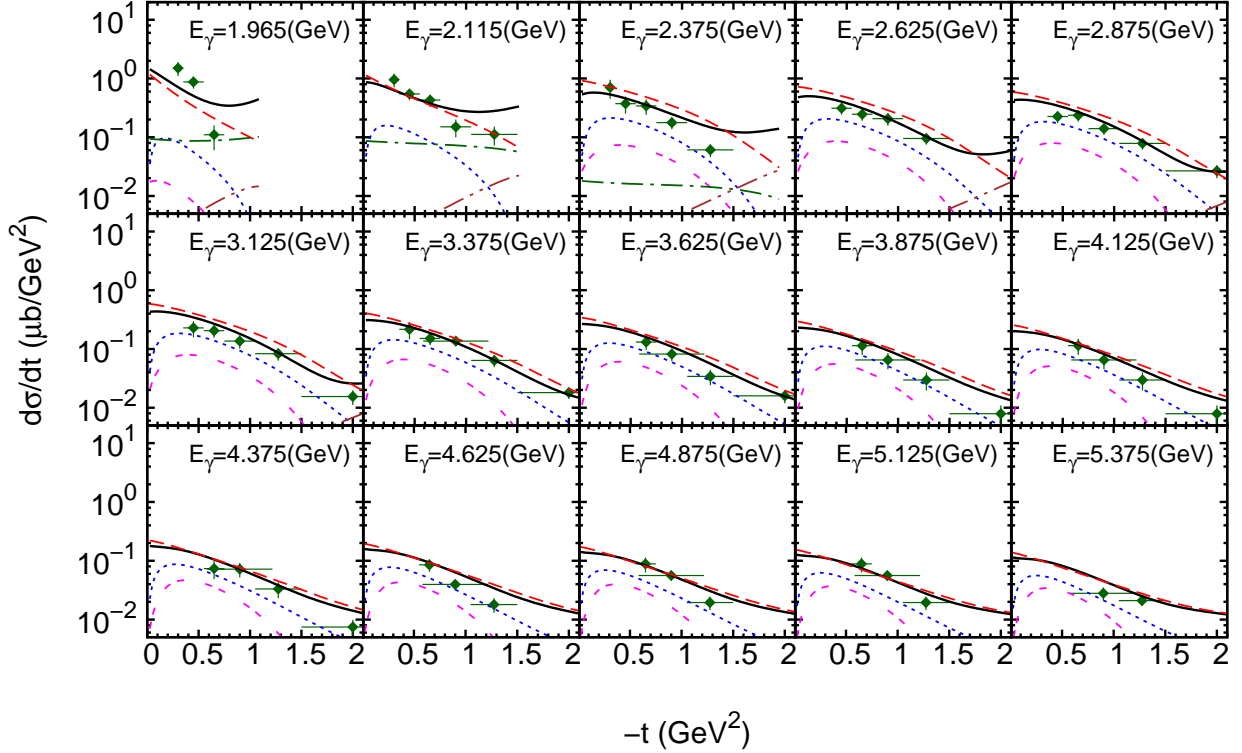


Figure 6: (Color online) The differential cross section  $d\sigma/dt$  with the variation of  $-t$ . The full diamond (darkgreen) and open square (cyan) are for the preliminary  $eg3$  data [29]. The notation as in Fig. 2

### 3.3. Total cross section

The total cross section can be obtained by integrating up the differential cross section. The uncertainties will be introduced in the extrapolation of the experimental differential cross section at measured angles to the values at all angles. Hence, we do not include the experimental total cross section in the fitting procedure. Our results calculated with the determined parameters are shown in Fig. 7 and compared with the experimental data. Besides the CLAS13 data, the old data by the SAPHIR experiment at the low energy [30] and the LAMP2 experiment at high energy [31] and preliminary  $eg3$  data are also presented. As shown in Fig. 7, our results are close to the experimental data. The contact term is dominant at all energies considered in the current work. The contribution from  $N(2120)$  is important at energies about 2.1 GeV.

## 4. Summary

To determine the interaction mechanism of the photoproduction of  $\Lambda(1520)$ , the high precision data with large range of kaon photoproduction angles are required. In this work we investigated the photoproduction of  $\Lambda(1520)$  in a Regge-plus-resonance approach based on the new high precision CLAS13 data. The result suggests that the contact terms are

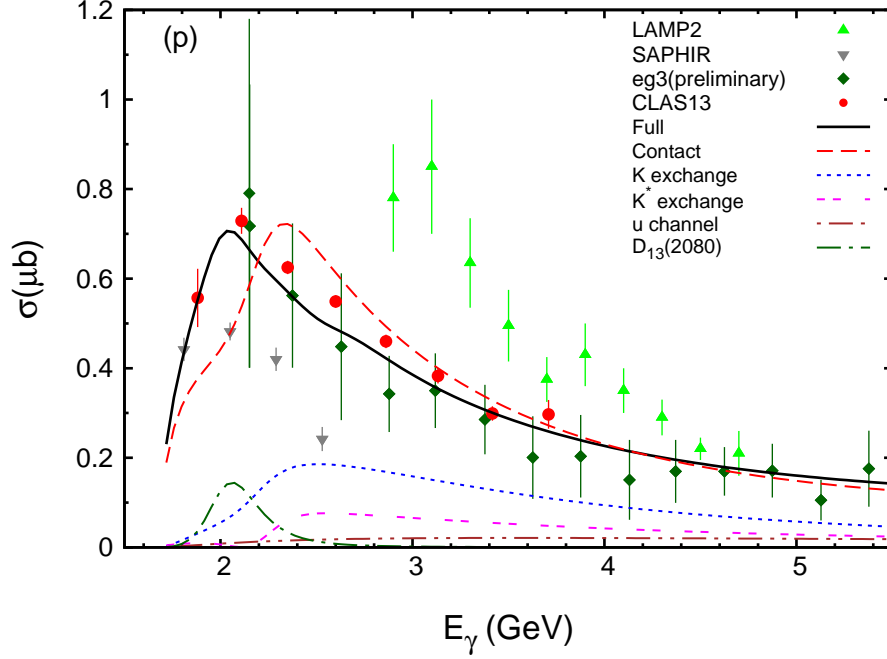


Figure 7: (Color online) Total cross section  $\sigma$  with the variation of the energy of photon  $E_\gamma$ . The notations for the theoretical results as in Fig. 2. The data are from Refs. [1, 29, 31, 30].

dominant in the photoproduction of  $\Lambda(1520)$ . The Regge trajectory is found essential to reproduce the experimental data at forward angles especially at high energies. To describe the behavior of the differential cross section at backward angles, the  $\Lambda$  intermediate  $u$  channel contribution should be included.

The nucleon resonance  $N(2120)$  with  $3/2^-$  is essential to reproduce the bump structure of near 2.1 GeV. In the new version of PDG [2], a state  $N(1875)$  with  $3/2^-$  is suggested. If the third  $[N_{\frac{3}{2}}^{\frac{3}{2}-}]_3$  state is set to  $N(1875)$ , the contribution from  $[N_{\frac{3}{2}}^{\frac{3}{2}-}]_3$  state with mass 1.875 GeV should be small considered the threshold of the  $\Lambda(1520)$  photoproduction about 2.01 GeV. Moreover, other nucleon resonances predicted in the constituent quark model have small contributions as shown in the current work. So, the assignment of  $[N_{\frac{3}{2}}^{\frac{3}{2}-}]_3$  as  $N(1875)$  will lead to a small  $D_{13}$  partial wave contribution in the  $\Lambda(1520)$  photoproduction. However, the results in this work and literatures [12,14] suggest that a  $D_{13}$  state about 2.1 GeV is essential to reproduce the experimental data. Hence, the  $[N_{\frac{3}{2}}^{\frac{3}{2}-}]_3$  should be assigned to  $N(2120)$ , not  $N(1875)$ .

## Acknowledgement

This project is partially supported by the Major State Basic Research Development Program in China (No. 2014CB845405), the National Natural Science Foundation of China (Grants No. 11275235, No. 11035006) and the Chinese Academy of Sciences (the Knowledge Innovation Project under Grant No. KJCX2-EW-N01).

## References

## References

- [1] K. Moriya *et al.* [CLAS Collaboration], Phys. Rev. C **88** (2013) 045201
- [2] J. Beringer et al. (Particle Data Group), Phys. Rev. D **86**, 010001 (2012) and 2013 partial update for the 2014 edition
- [3] A. V. Anisovich, R. Beck, E. Klempt, V. A. Nikonov, A. V. Sarantsev and U. Thoma, Eur. Phys. J. A **48** (2012) 15 [arXiv:1112.4937 [hep-ph]].
- [4] S. Capstick and W. Roberts, Phys. Rev. D **58**, 074011 (1998)
- [5] S. Capstick, Phys. Rev. D **46**, 2864 (1992).
- [6] S. -H. Kim, S. -i. Nam, Y. Oh and H. -C. Kim, Phys. Rev. D **84**, 114023 (2011)
- [7] A. Kiswandhi and S. N. Yang, Phys. Rev. C **86** (2012) 015203 [Erratum-ibid. C **86** (2012) 019904]
- [8] J. F. Zhang, N. C. Mukhopadhyay and M. Benmerrouche, Phys. Rev. C **52**, 1134 (1995)
- [9] K. Nakayama and H. Haberzettl, Phys. Rev. C **73**, 045211 (2006)
- [10] X. -H. Zhong and Q. Zhao, Phys. Rev. C **84**, 065204 (2011)
- [11] J. He, B. Saghai Phys. Rev. C **80**, 015207 (2009)
- [12] H. Kohri *et al.* [LEPS Collaboration], Phys. Rev. Lett. **104**, 172001 (2010) [arXiv:0906.0197 [hep-ex]].
- [13] J. J. Xie and J. Nieves, Phys. Rev. C **82**, 045205 (2010)
- [14] J. He and X. -R. Chen, Phys. Rev. C **86** (2012) 035204
- [15] J. -J. Xie, E. Wang and J. Nieves, arXiv:1309.7135 [nucl-th].
- [16] J. He, arXiv:1311.0571 [nucl-th].
- [17] S. I. Nam and C. W. Kao, Phys. Rev. C **81**, 055206 (2010)
- [18] H. Haberzettl, K. Nakayama and S. Krewald, Phys. Rev. C **74**, 045202 (2006)
- [19] Y. Oh, C. M. Ko, K. Nakayama, Phys. Rev. **C77**, 045204 (2008).
- [20] M. Warns, W. Pfeil and H. Rollnik, Phys. Lett. B **258** (1991) 431.
- [21] M. Guidal, J. M. Laget and M. Vanderhaeghen, Nucl. Phys. A **627**, 645 (1997).
- [22] T. Corthals, T. Van Cauteren, J. Ryckebusch and D. G. Ireland, Phys. Rev. C **75**, 045204 (2007)
- [23] A. I. Titov, B. Kampf, S. Date and Y. Ohashi, Phys. Rev. C **72**, 035206 (2005) [Erratum-ibid. C **72**, 049901 (2005)]
- [24] H. Toki, C. Garcia-Recio and J. Nieves, Phys. Rev. D **77**, 034001 (2008)
- [25] S. -J. Chang, Phys. Rev. **161**, 1308 (1967).
- [26] J. G. Rushbrooke, Phys. Rev. **143**, 1345 (1966).
- [27] R. E. Behrends and C. Fronsda Phys. Rev. **106**, 345 (1957).
- [28] N. Muramatsu *et al.*, Phys. Rev. Lett. **103**, 012001 (2009)
- [29] Zhiwen Zhao, Presented at the 8th Workshop on the Physics of Excited Nucleons (NSTAR2011), Newport News, USA, May 2011
- [30] F. W. Wieland, *et al.*, arXiv:1011.0822 [nucl-ex].
- [31] D. P. Barber *et al.*, Z. Phys. C **7**, 17 (1980).